Electronic Supplementary Information for

Nitrogen-doped Ru film for energy-saving hydrogen production assisted with hydrazine oxidation

Ziqiang Wang, Xian Zhang, Wenjing Tian, Hongjie Yu, Kai Deng, You Xu, Xin Wang, Hongjing Wang* and Liang Wang*

State Key Laboratory Breeding Base of Green-Chemical Synthesis Technology, College of Chemical Engineering, Zhejiang University of Technology, Hangzhou 310014, P. R. China

Corresponding authors

*E-mails: hjw@zjut.edu.cn, wangliang@zjut.edu.cn

Experimental Section

Chemicals and Materials: Poly(ethylene oxide)-*b*-Poly(methyl methacrylate) (PEO-*b*-PMMA) block copolymer was ordered from Polymer Source Inc. Ruthenium (III) chloride hydrate ($RuCl_3 \cdot xH_2O$) was ordered from Sigma-Aldrich. Commercial IrO_2 and Pt/C (20 wt%) were supplied by Alfa Aesar. Hydrazine monohydrate ($N_2H_4 \cdot H_2O$), ethanol (C_2H_5OH), potassium hydroxide (KOH), tetrahydrofuran (THF), hydrochloric acid (HCl, 36−38%) were ordered from Aladdin.

Synthesis of N-mRu/NF: The mRu/NF was first synthesized via electrodeposition. Typically, PEO-*b*-PMMA (5 mg) was dissolved in THF (0.5 mL) under sonication for 30 min, followed by adding $RuCl_3$ (0.5 mL, 40 mM) and water (3.5 mL), which was used as electrolyte. The electrodeposition was conducted by CHI 660E electrochemical workstation at −0.6 V for 6000 s in three-electrode cell using Ag/AgCl (saturated KCl) electrode, Pt wire and pretreated NF as the reference, counter and working electrodes, respectively. After washing with water and ethanol, the mRu/NF was obtained. Finally, the mRu/NF was placed in a tube furnace and annealed in NH_3 atmosphere for 2 h at 300 °C with a heating rate of 2 °C min^{-1}.

Characterizations: Scanning electron microscopy (SEM, ZEISS SUPRA 55) and transmission electron microscopy (TEM, JEOL JEM-2010) were used to analyze morphology and microstructure of samples. The crystallographic data of samples were analyzed by X-ray diffraction (XRD) on a DX-2700 diffractometer. X-ray photoelectron spectroscopy (XPS) spectra were gathered on a Thermo Scientific K-Alpha (Kratos Analytical). All the binding energies were calibrated to C 1s adventitious carbon at 284.8 eV to eliminate differences in sample charging.

Electrochemical measurements: Electrochemical experiments were performed under ambient conditions using conventional three-electrode system, where the obtained sample was working electrode, graphite rod was counter electrode, and Hg/HgO electrode was reference electrode. The HER and HzOR electrolytes were 1.0 M KOH and 1.0 M KOH + 0.5 M N_2H_4, respectively. The potential was scaled to reference reversible hydrogen electrode (RHE). Linear scanning voltammetry (LSV) was performed at 5 mV s^{-1}. Electrochemical impedance spectroscopy (EIS) was carried out between 100 kHz and 100 mHz.

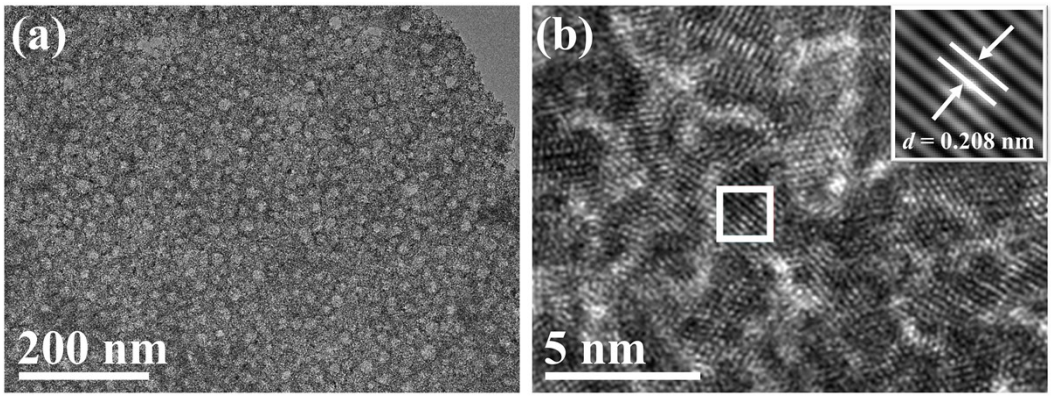

Fig. S1 (a) TEM and (b) HRTEM images of the mRu film. The inset in (b) is the corresponding Fourier-filtered lattice stripes.

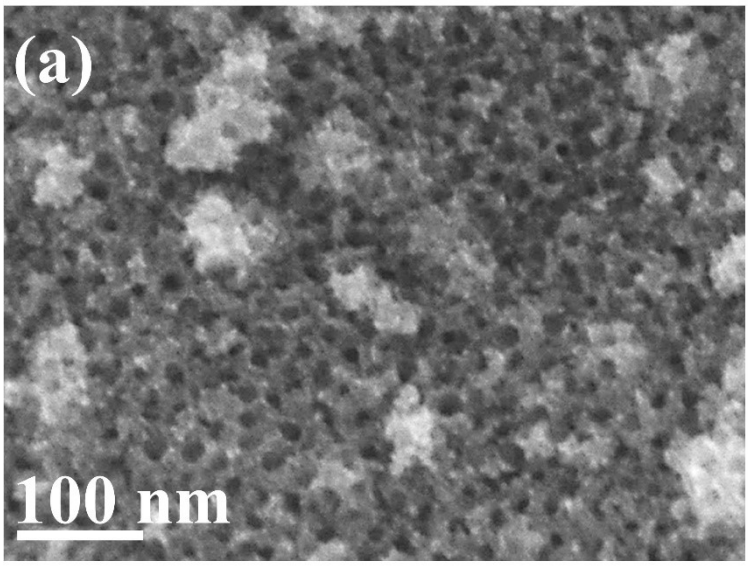

Fig. S2 (a) SEM image of N-mRu/NF.

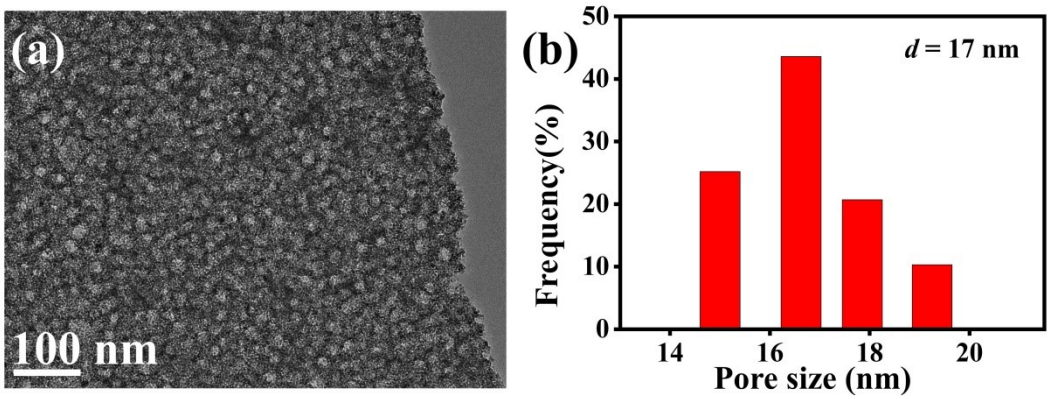

Fig. S3 (a) TEM image and (b) pore size distribution of the N-mRu film.

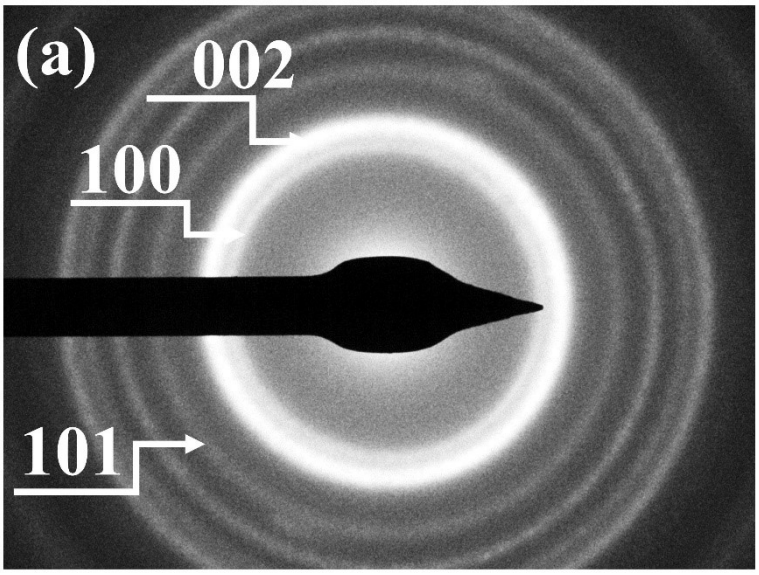

Fig. S4 SAED pattern of N-mRu flim.

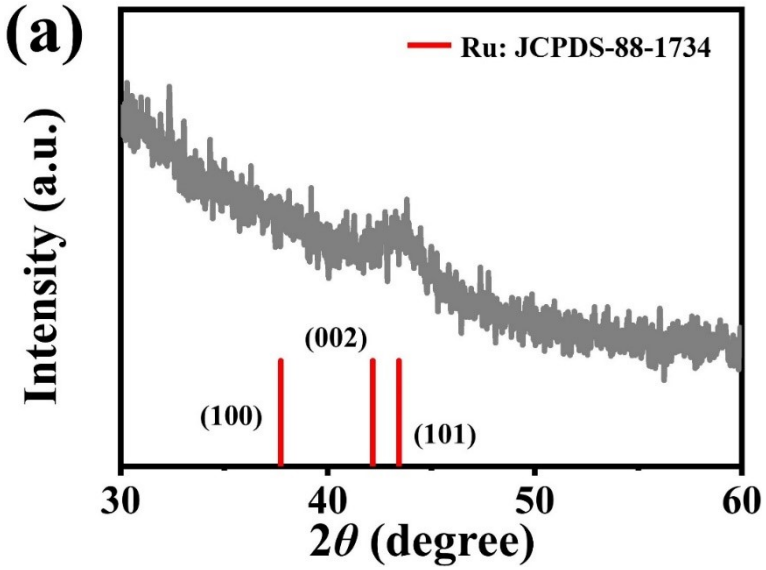

Fig. S5 XRD pattern of mRu film after N_2 annealling.

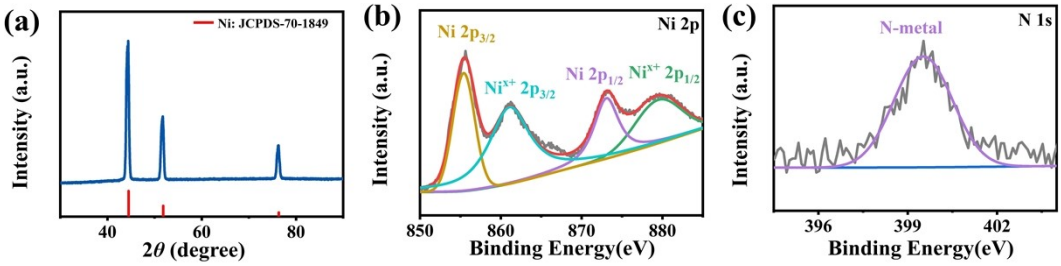

Fig. S6 (a) XRD pattern and XPS spectra of (b) Ni 2p and (c) N 1s for N-NF.

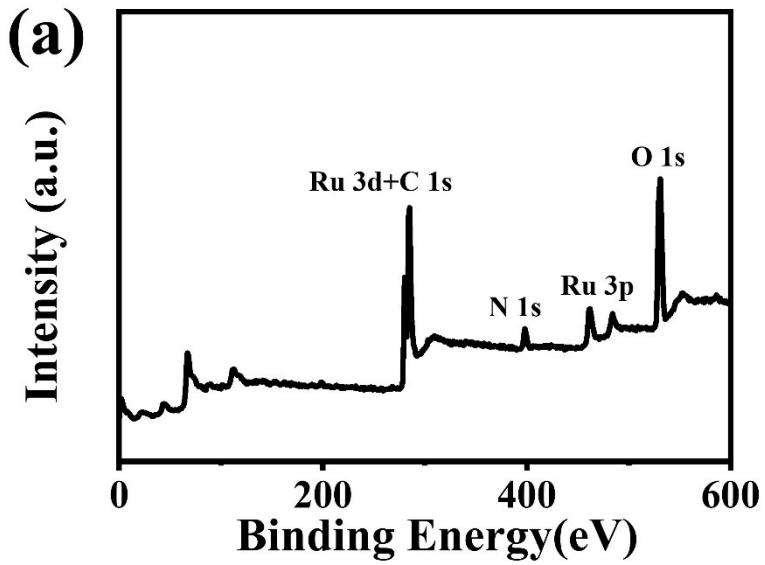

Fig. S7 XPS survey spectrum of N-mRu/NF.

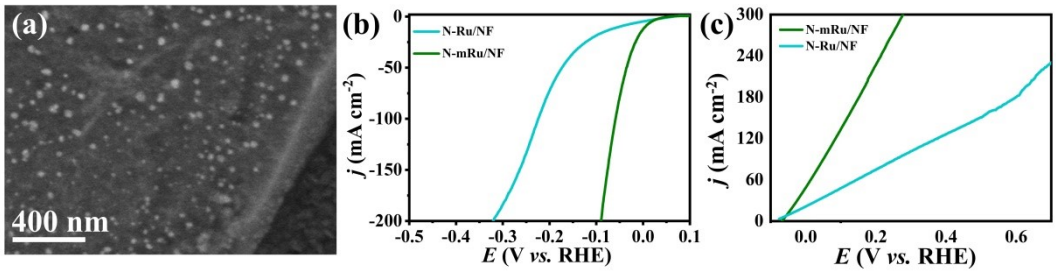

Fig. S8 (a) SEM image of the N-Ru/NF and its LSV curves in (b) 1.0 M KOH and (c) 1.0 M KOH + 0.5 M N_2H_4.

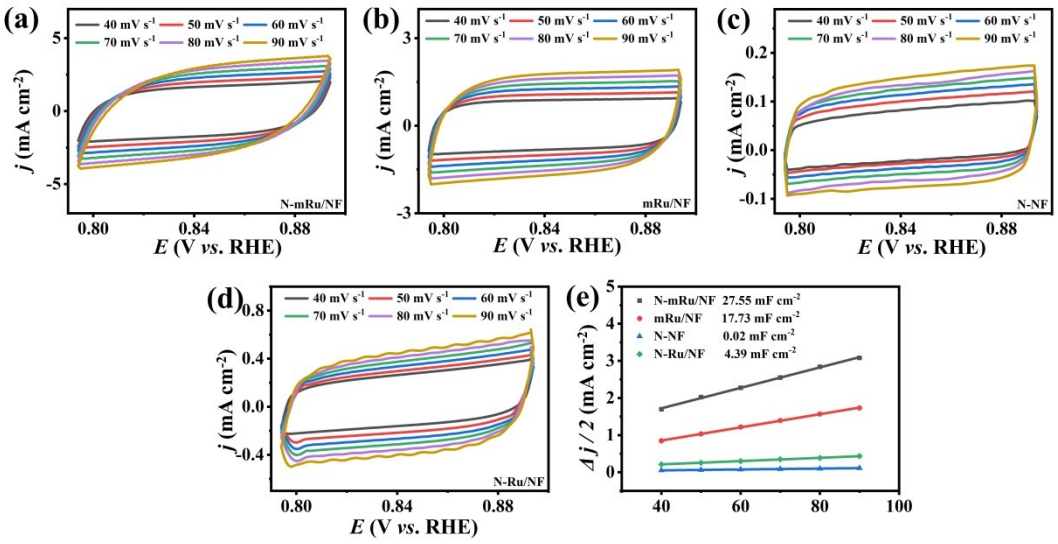

Fig. S9 CV curves of different samples in the range of 0.794 to 0.894 V and corresponding fitted plots.

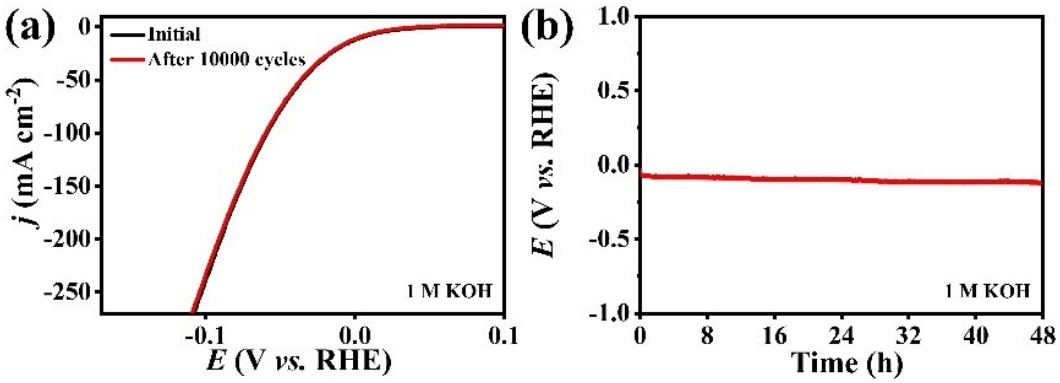

Fig. S10 (a) LSV curves of N-mRu/NF before and after 10,000 CV cycles. (b) Long-term stability test at −20 mA cm^{-2}.

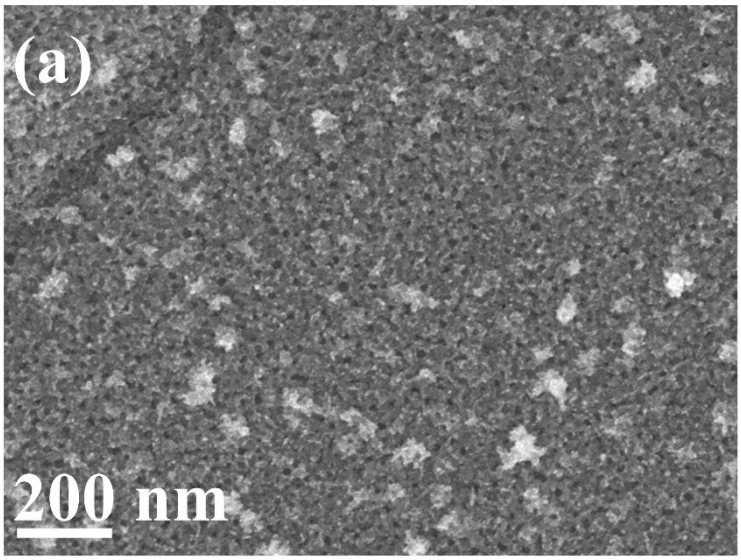

Fig. S11 SEM image of N-mRu/NF after HER stability test.

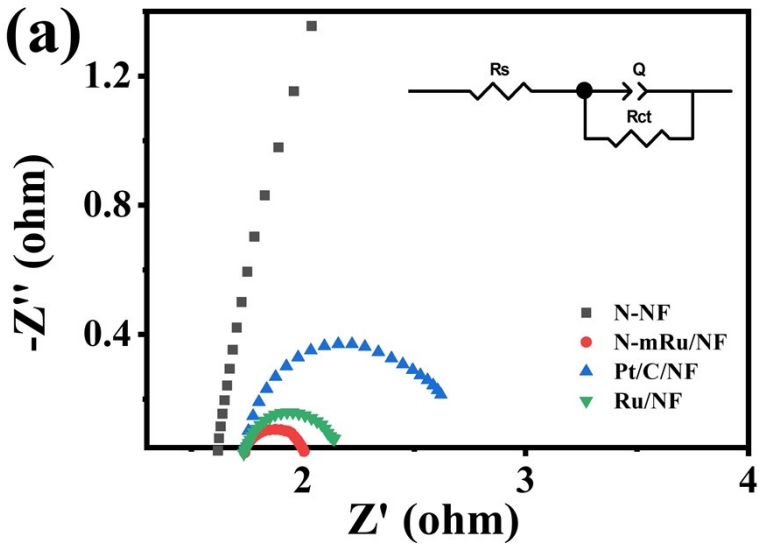

Fig. S12 EIS spectra of samples at 0.044 V in 1.0 M KOH + 0.5 M N_2H_4.

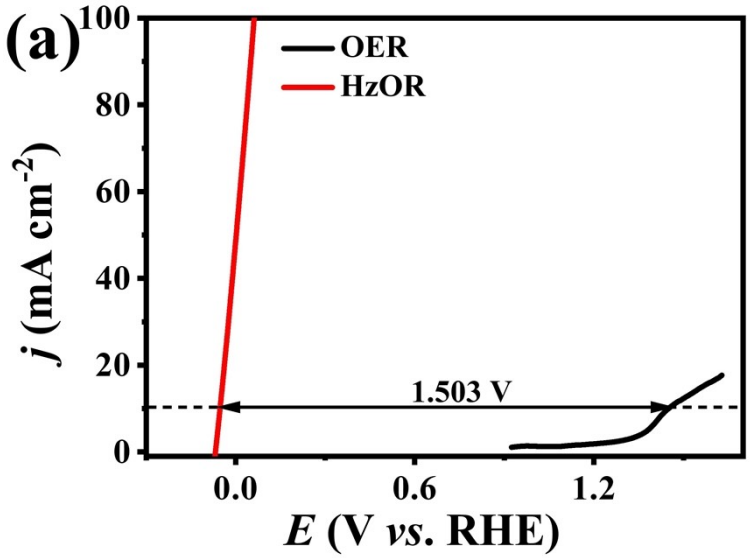

Fig. S13 LSV curves of N-mRu/NF for OER and HzOR.

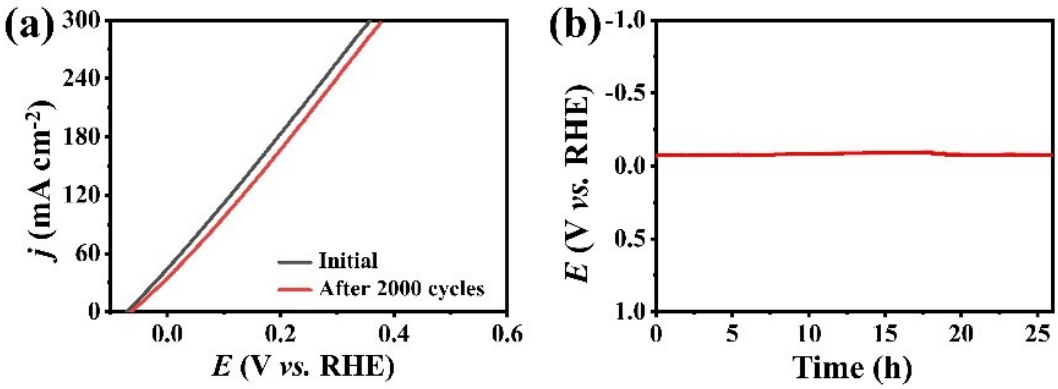

Fig. S14 (a) HzOR polarization curves of N-mRu/NF before and after 2000 CV cycles. (b) Long-term stability test at 10 mA cm^{-2}.

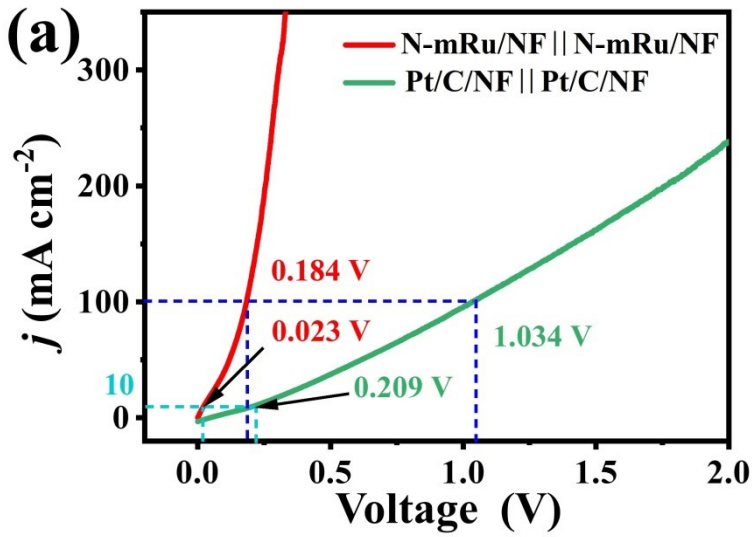

Fig. S15 LSV curves of N-mRu/NF||N-mRu/NF and Pt/C/NF||Pt/C/NF systems for overall hydrazine electrolysis.

Table S1. Summary of the representative reports on electrocatalytic HER at ambient conditions

Catalyst	Electrolyte	Overpotential	Ref.
N-mRu/NF	**1 M KOH**	**-60 mV at -100 mA cm^{-2}**	**This work**
NF/mRh@PANI	1 M KOH	-69 mV at -100 mA cm^{-2}	1
Pt-$Co(OH)_2$/CC	1 M KOH	-122 mV at -100 mA cm^{-2}	2
PdS NSs	1 M KOH	-233 mV at -100 mA cm^{-2}	3
Ru-TA /ACC	1 M KOH	-95 mV at -50 mA cm^{-2}	4
$RuSe_2$	1 M KOH	-90.1 mV at -100 mA cm^{-2}	5
RhPx@NPC	1 M KOH	-69 mV at -10 mA cm^{-2}	6
$CoSe_2$/$MoSe_2$	1 M KOH	-168 mV at -10 mA cm^{-2}	7
Rh/N-CBs	1 M KOH	-77 mV at -10 mA cm^{-2}	8
RuP_2@NPC	1 M KOH	-52 mV at -10 mA cm^{-2}	9
PdH-NDs	1 M KOH	-358 mV at -10 mA cm^{-2}	10

Table S2. Summary of the representative reports on electrocatalytic HzOR at ambient conditions

Catalyst	Electrolyte	Overpotential (V) at 10 mA cm^{-2}	Ref.
N-mRu/NF	**1 M KOH+0.5 M N_2H_4**	**-0.052**	**This work**
Rh_2S_3/NC	1 M KOH +0.1 M N_2H_4	0.095	11
Mo–Ni_3N/Ni/NF	1 M KOH +0.1 M N_2H_4	-0.0003	12
Cu_1Ni_2-N	1 M KOH +0.5 M N_2H_4	0.0005	13
$NiFe(OH)_2$-SD/NF	1 M KOH +0.5 M N_2H_4	0.06	14
Ni NCNA	1 M KOH +0.3 M N_2H_4	-0.026	15
RhIr MNs	1 M KOH +0.5 M N_2H_4	-0.012	16
$CoSe_2$	1 M KOH+0.5 M N_2H_4	-0.017	17
PW-Co_3N	1 M KOH +0.1 M N_2H_4	-0.055	18
Ni (Cu)@NiFeP/NM	1 M KOH+0.5 M N_2H_4	0.117	19

References

1. Z. Y. Duan, K. Deng, C. J. Li, M. Zhang, Z. Q. Wang, Y. Xu, X. N. Li, L. Wang and H. J. Wang, *Chem. Eng. J.*, 2022, **428**, 132646.
2. Z. Xing, C. Han, D. Wang, Q. Li and X. Yang, *ACS Catal.*, 2017, **7**, 7131-7135.
3. Y. Wang, K. Xu, Z. Zhu, W. Guo, T. Yu, M. He, W. Wei and T. Yang, *Chem. Commun.*, 2021, **57**, 1368-1371.
4. J. Chen, H. Wang, Y. Gong and Y. Wang, *J. Mater. Chem. A*, 2019, **7**, 11038-11043.
5. Z. Zhang, C. Jiang, P. Li, K. Yao, Z. Zhao, J. Fan, H. Li and H. Wang, *Small*, 2021, **17**, 2007333.
6. J. Q. Chi, X. J. Zeng, X. Shang, B. Dong, Y. M. Chai, C. G. Liu, M. Marin and Y. Yin, *Adv. Funct. Mater.*, 2019, **29**, 1901790.
7. X. Tang, J.-Y. Zhang, B. Mei, X. Zhang, Y. Liu, J. Wang and W. Li, *Chem. Eng. J.*, 2021, **404**, 126529.
8. N. Jia, Y. Liu, L. Wang, P. Chen, X. Chen, Z. An and Y. Chen, *ACS Appl. Mater. Interfaces*, 2019, **11**, 35039-35049.
9. Z. Pu, I. S. Amiinu, Z. Kou, W. Li and S. Mu, *Angew. Chem., Int. Ed.*, 2017, **56**, 11559-11564.
10. H. Y. Sun, Y. Ding, Y. Q. Yue, Q. Xue, F. M. Li, J. X. Jiang, P. Chen and Y. Chen, *ACS Appl. Mater. Interfaces*, 2021, **13**, 13149-13157.
11. C. Zhang, H. Liu, Y. Liu, X. Liu, Y. Mi, R. Guo, J. Sun, H. Bao, J. He, Y. Qiu, J. Ren, X. Yang, J. Luo and G. Hu, *Small Methods*, 2020, **4**, 2000208.
12. Y. Liu, J. Zhang, Y. Li, Q. Qian, Z. Li and G. Zhang, *Adv. Funct. Mater.*, 2021, **31**, 2103673.

13. Z. Wang, L. Xu, F. Huang, L. Qu, J. Li, K. A. Owusu, Z. Liu, Z. Lin, B. Xiang, X. Liu, K. Zhao, X. Liao, W. Yang, Y. B. Cheng and L. Mai, *Adv. Energy Mater.*, 2019, **9**, 1900390.

14. P. Babar, A. Lokhande, V. Karade, I. J. Lee, D. Lee, S. Pawar and J. H. Kim, *J. Colloid Interface Sci.*, 2019, **557**, 10-17.

15. Y. Li, J. Li, Q. Qian, X. Jin, Y. Liu, Z. Li, Y. Zhu, Y. Guo and G. Zhang, *Small*, 2021, **17**, 2008148.

16. M. Zhang, Z. Wang, Z. Duan, S. Wang, Y. Xu, X. Li, L. Wang and H. Wang, *J. Mater. Chem. A*, 2021, **9**, 18323-18328.

17. J. Y. Zhang, H. Wang, Y. Tian, Y. Yan, Q. Xue, T. He, H. Liu, C. Wang, Y. Chen and B. Y. Xia, *Angew. Chem., Int. Ed.*, 2018, **57**, 7649-7653.

18. Y. Liu, J. Zhang, Y. Li, Q. Qian, Z. Li, Y. Zhu and G. Zhang, *Nat. Commun.*, 2020, **11**, 1853.

19. Q. Sun, M. Zhou, Y. Shen, L. Wang, Y. Ma, Y. Li, X. Bo, Z. Wang and C. Zhao, *J. Catal.*, 2019, **373**, 180-189.